Time-Resolved FTIR Studies of the GTPase Reaction of H-*Ras* P21 Reveal a Key Role for the β-Phosphate[†]

V. Cepus,[‡] A. J. Scheidig,[§] R. S. Goody,[§] and K. Gerwert*,[‡]

Lehrstuhl für Biophysik, Fakultät Biologie, Ruhr-Universität, ND04, D-44780 Bochum, Germany, and Max-Planck-Institut für molekulare Physiologie, Rheinlanddamm 201, D-44139 Dortmund, Germany

Received December 30, 1997; Revised Manuscript Received March 26, 1998

ABSTRACT: FTIR difference spectroscopy has been established as a new tool to study the GTPase reaction of H-*ras* p21 (Ras) in a time-resolved mode at atomic resolution without crystallization. The phosphate vibrations were analyzed using site specifically ^{18}O-labeled caged GTP isotopomers. One nonbridging oxygen per nucleotide was replaced for an ^{18}O isotope in the α-, β-, or γ-position of the phosphate chain. In photolysis experiments with free caged GTP, strong vibrational coupling was observed among all phosphate groups. The investigation of Ras•caged GTP photolysis and the subsequent hydrolysis reaction of Ras•GTP showed that the phosphate vibrations are largely decoupled by interaction with the protein in contrast to free GTP. The characteristic isotope shifts allow band assignments to isolated α-, β-, and γ-phosphate vibrations of caged GTP, GTP, and the liberated inorganic phosphate. The unusually low frequency of the β (PO_2^-) vibration of Ras-bound GTP, as compared to free GTP, indicates a large decrease in the P−O bond order. The bond order decrease reveals that the oxygen atoms of the β (PO_2^-) group interact much more strongly with the protein environment than the γ-oxygen atoms. Thereby, electrons are withdrawn from the β-phosphorus, and thus also from the β/γ-bridging oxygen. This leads to partial bond breakage or at least weakening of the bond between the β/γ-bridging oxygen and the γ-phosphorus atom as a putative early step of the GTP hydrolysis. Based on these results, we propose a key role of the β-phosphate for GTP hydrolysis. The assignments of phosphate bands provide a crucial marker for further time-resolved FTIR studies of the GTPase reaction of Ras.

The human proto-oncogene protein product H-*ras* p21 (Ras)[1] acts as a timer switch in such important processes as cell differentiation and proliferation. Stimulation of specific receptors leads to the replacement of tightly bound GDP for GTP induced by specific exchange factors (*1*, *2*). The "active" GTP bound state initiates a kinase cascade which results in a transcriptional response (*3*). With an intrinsic GTPase rate of 0.028 min^{-1} at 37 °C, Ras•GTP returns to the "inactive" Ras•GDP state while it releases inorganic phosphate (*4*−*6*). This rate can be accelerated considerably by GTPase activating proteins (GAPs) (*7*).

If the GTPase reaction is slowed by mutation of a critical residue in the active site, the signal transduction pathway becomes permanently activated. In this manner, single point mutations in the amino acid positions 12, 13, and 61 lead to oncogenic Ras. In fact, Ras mutations appear to be involved in ca. 30% of all human tumors (*8*, *9*). Since the signal transduction pathways of Ras proteins have been well examined, this system is potentially a promising field for pharmaceutical applications (*10*).

The three-dimensional structure of Ras with the slowly hydrolyzing GTP analogue GppNHp has been determined at 1.35 Å resolution (*11*, *12*). This structure is thought to mimic very closely the active GTP bound state of Ras. A water molecule which is considered to attack the γ-phosphate of the bound GTP has been identified in this crystal structure. However, although these results provide an excellent basis for interpretation, the molecular GTPase mechanism is still not yet clear. Several proposed GTPase mechanisms suggest an associative transition state. For such a nucleophilic substitution (analogous to an S_{N2} type reaction), water is not considered to be nucleophilic enough as an attacking agent. A general base is thought to be needed to abstract a proton and activate the water molecule. This water molecule, identified in the Ras•GppNHp structure, is hydrogen bonded with the backbone C═O of Thr-35 and in one possible configuration with the side chain carbamoyl group of Gln-61. This amino acid was therefore the initial candidate for the general base which activates the water for nucleophilic attack (*13*, *14*). However, the low p*K* value of this group is considered to be inconsistent with such a role of the glutamine side chain, although it should be pointed out that in the proposed mechanism this situation would be somewhat ameliorated by interaction of the Gln-61 and Glu-63 side chains. However, the introduction of an unnatural "nitro

[†] This work was supported by the Deutsche Forschungsgemeinschaft, SFB-394-B1.

* Author to whom correspondence should be addressed. Phone: ++49-234-700-4461. Fax: ++49-234-709-4238.

[‡] Ruhr-Universität.

[§] Max-Planck-Institut für Molekulare Physiologie.

[1] Abbreviations: GTP, guanosine-5′-triphosphate; GppNHp, guanosine-5′-(β/γ-imido-)triphosphate; caged GTP, P^3-[1-(2-nitrophenyl)-ethyl]guanosine-5′-triphosphate, H-*ras* p21 or Ras, H-*ras* p21 (1−166: carboxy terminally truncated); GAP, GTPase activating protein; ONAP, *o*-nitroso acetophenone.

S0006-2960(97)03183-8 CCC: $15.00
Published on Web 06/20/1998

Scheme 1: Reaction Scheme of the Investigated Reactions[a]

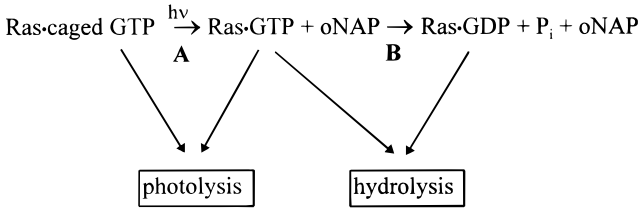

[a] Photolysis of Ras•caged GTP (reaction A), GTP hydrolysis of Ras•GTP (reaction B).

glutamine" in position 61, with a side chain which is an even weaker base than that of Gln, led to an essentially unchanged GTPase activity, so that the role of Gln-61 as a general base was excluded (*15*), at least for the nonactivated GTPase (i.e., without GAP). A more likely general base now appears to be the γ-phosphate itself, in a mechanism which has been called substrate assisted catalysis (*16*). Gln-61 appears to stabilize the transition state in the GAP activated mechanism. This has been confirmed by crystal structure data of Ras•GAP-334 where bound GDP•AlF_3 or GDP•AlF_4^- mimics an intermediate close to the transition state of the GTPase reaction (*17*). The same observation was made for the crystal structure of the RhoA•RhoGAP complex which could be stabilized in an analogous way (*18*). A similar role of an equivalent glutamine residue was also found in analogous crystal structures of $G_{t\alpha}$ and $G_{i\alpha}$ for Gln-200 and Gln-204, respectively, which are homologous to Gln-61 in Ras (*19*, *20*). In contrast, a dissociative GTP hydrolysis mechanism (S_{N1} type) has also been suggested, extrapolating from solution studies on the nonenzymatic hydrolysis of GTP (*21*). An analogy was driven to the GTPase reaction of Ras and several arguments for a dissociative mechanism were found by the authors from the crystal structure data of Ras.

For a detailed investigation of the GTPase mechanism of Ras we chose as an approach time-resolved FTIR difference spectroscopy. This method allows the determination of molecular reaction mechanisms of proteins at the atomic level, in a time-resolved mode, and in solution (*22*). The method has been applied successfully to bacteriorhodopsin (*23*) and photosynthetic reaction centers (*24*). So far, time-resolved FTIR spectroscopy was limited to photobiological systems using the intrinsic chromophores for the initiation of the protein reaction at the desired point in time.

For the investigation of the small GTPase Ras, the use of photolabile GTP precursors as P^3-[1-(2-nitrophenyl)ethyl] guanosine 5′-triphosphate (caged GTP) has been applied successfully (*25*). Caged GTP is not a substrate, but is tightly bound to Ras (*26*, *27*). Using an intense UV laser flash, caged GTP can be photolyzed, Ras-bound GTP is liberated, and the GTPase reaction can be observed in a time-resolved mode with infrared spectroscopy (Scheme 1). Fortunately, the photolysis of Ras•caged GTP (reaction A) is fast ($t_{1/2}$ is ca. 100 ms at 30 °C and pH 7.5) with respect to the GTPase reaction of Ras•GTP (reaction B, $t_{1/2} \approx 60$ min at the same conditions). Therefore, these reactions can be separated kinetically. By using ^{18}O-labeled caged GTP, the phosphate bands of Ras•caged GTP, Ras•GTP, Ras•GDP, and inorganic phosphate are assigned and implications for the GTPase mechanism are drawn.

MATERIALS AND METHODS

P^3-[1-(2-nitrophenyl)ethyl] guanosine 5′-triphosphate (caged GTP) and P^3-[1-(2-nitrophenyl)ethyl] guanosine 5′-*O*-(γ-thio) triphosphate (caged GTPγS) were synthesized following the procedure of Walker (*28*) by esterification of guanosine 5′-*O*-triphosphate (GTP) and the γS analogue guanosine 5′-*O*-(γ-thio) triphosphate (GTPγS, Merck), respectively, with 1-(2-nitrophenyl)diazoethane. The ^{18}O-labeled isotopomers were prepared starting with the sulfur analogues guanosine 5′-*O*-(α-thio) triphosphate (GTPαS), guanosine 5′-*O*-(β-thio) triphosphate (GTPβS), and P^3-[1-(2-nitrophenyl)ethyl] guanosine 5′-*O*-(γ-thio) triphosphate (caged GTPγS) by oxidation with *N*-chlorosuccinimide and hydrolysis with $H_2{}^{18}O$ (*29*). Guanosine 5′-*O*-(α-^{18}O) triphosphate (GTPα^{18}O) and guanosine 5′-*O*-(β-^{18}O) triphosphate (GTP$\beta^{18}O$) were then esterified with 1-(2-nitrophenyldiazoethane) as described above.

An excess of the desired caged GTP isotopomer in the presence of alkaline phosphatase was used to replace the GDP which is initially bound to Ras (*30*). The excess of unbound caged GTP was subsequently removed by gel filtration chromatography. FTIR measurements were performed in 100 mM HEPES, 50 mM $MgCl_2$, and 25 mM caged GTP at pH 7.5 for photolysis measurements without protein. The concentrations in the experiments with Ras are 50 mM HEPES, 25 mM $MgCl_2$, 10 mM dithiothreitol (DTT), and 10 mM 1:1 complex Ras•caged GTP at pH 7.5.

The sample solution was pressed between two CaF_2 windows of 20 mm diameter. The distance between these windows was held at about 2.5 μm by a Mylar spacer. A metal cuvette fixed the sample in the spectrometer, and the sample holder could be stabilized at the temperature of choice. All spectra in the absence of Ras were recorded at 295 K, the spectra in the presence of Ras at 303 K. A somewhat increased temperature was used in the protein-bound case, as compared to the photolysis experiments with caged GTP, to accelerate the slow intrinsic hydrolysis rate to prevent baseline distortions due to longer measurement times. However, at higher temperatures the protein becomes less stable. The temperature of 303 K was the most appropriate compromise. The spectra are presented between 1800 and 1000 cm^{-1}. Above 1800 cm^{-1}, no clear bands are observed, and below 1000 cm^{-1} the CaF_2 window absorbs strongly.

To visualize only bands of those groups undergoing reactions beyond the large background absorbance of the protein, difference spectra between the ground state and an activated state were calculated. Photolysis was performed with the excimer lasers EMG101 or LPX240 (Lambda Physics) at 308 nm. The laser energy chosen was between 100 and 200 mJ per flash with a pulse duration of about 20 ns. Twenty to 50 flashes were used to achieve complete conversion of caged GTP. The first flash converts up to ca. 10% of caged GTP. The exact number of flashes required for a photolysis yield of 90% was determined in a control experiment; free caged GTP was photolyzed by several flashes until saturation occurred when plotting the absorbance change of the marker bands at 1526 and 1346 cm^{-1} against the number of flashes. Subsequently, the exact amount of released GTP was determined by HPLC analysis and the saturation curve was normalized.

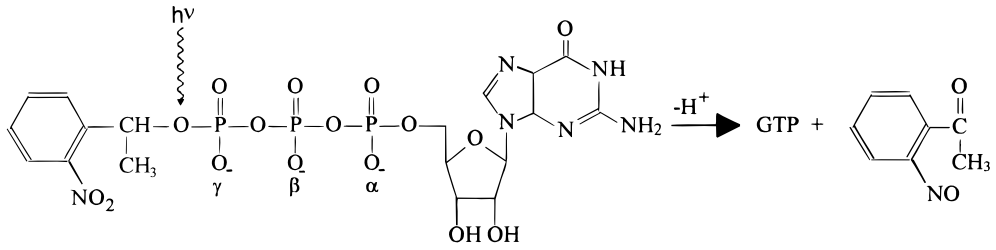

FIGURE 1: Photolysis reaction of P^3-[1-(2-nitrophenyl)ethyl] guanosine 5′-triphosphate (caged GTP). By an intense UV flash, GTP and *o*-nitroso acetophenone (ONAP) are released. ONAP is captured by DTT. The position of the ^{18}O label: isotopomer **1**, unlabeled; **2**, one ^{18}O isotope at position α; **3**, one ^{18}O isotope at position β; **4**, one ^{18}O isotope at position γ. The resulting GTP isotopomers obtained by photolysis are termed **1′**, **2′**, **3′**, and **4′**.

FTIR spectra were collected on a IFS88 or IFS66v spectrometer (Bruker) equipped with a mercury cadmium telluride detector (MCT) between 1975 and 900 cm^{-1} with spectral resolution of 4 cm^{-1}. A more detailed description of the experimental setup can be found elsewhere (*31*−*33*). Each spectrum was an average of 1000 interferometer scans. The duration for the acquisition and calculation of one spectrum was 110 s. During the GTPase reaction of Ras•GTP spectra were collected up to 200 min after photolysis.

The first spectrum after photolysis of Ras•caged GTP represents the reference spectrum for Ras•GTP. Since the half-life of the GTPase reaction is about 60 min at 30 °C under the conditions used and the mean acquisition time of the spectrum taken directly after the photolysis is 55 s, less than 2% of the Ras•GTP was converted into Ras•GDP and inorganic phosphate. Biochemical investigations in solution yield a monophasic decay of the Ras•GTP complex with a rate constant of 0.028 min^{-1} at 37 °C (*4*). The values are essentially unchanged even under the very high protein concentrations used in the FTIR measurements.

The conversion of caged GTP to GTP or GDP was monitored after each experiment by HPLC. The sample was diluted with water and separated on a reverse phase column.

RESULTS AND DISCUSSION

In the present study the phosphate absorption (1300−900 cm^{-1}) was analyzed by use of the four isotopomers caged GTP, **1**; caged GTPα^{18}O, **2**; caged GTP$\beta^{18}O$, **3**; and caged GTP$\gamma^{18}O$, **4** (Figure 1). In former experiments the protein-free caged GTP isotopomers were examined (*33*). Here, the photolysis spectra of Ras-bound isotopomeric nucleotides caged GTP, **1**, **2**, **3**, and **4**, and the hydrolysis spectra arising from the subsequent GTPase reaction of Ras•GTP with bound isotopomeric GTP, **1′**, **2′**, **3′**, and **4′**, were analyzed.

Photolysis of Caged GTP−Mg^{2+}. Caged GTP was photolyzed using 20 ns laser pulses at $\lambda = 308$ nm, and FTIR difference spectra were recorded. The difference between the spectra of the photolyzed and unphotolyzed sample is shown in Figure 2a. The positive bands represent product, and the negative band educt vibrations. The detailed analysis of the photolysis spectra is described in (*33*). The band at 1346 cm^{-1} is assigned to the symmetric N−O valence vibration of the nitro group of caged GTP, respectively (*33*). This band can be used as indicator for the amount of photolyzed GTP.

Below 1300 cm^{-1}, the spectra are dominated by the phosphate vibrations. Bond cleavage between the cage moiety and GTP leads to a negative band at 1273 cm^{-1}. It is assigned to the asymmetric stretching vibration of the γ (PO_2^-) group to which the caging group is attached (34−35). On photolysis, the γ (PO_2^-) group is converted to the terminal γ (PO_3^{2-}) group of the released GTP. The degenerate stretching vibration of the γ (PO_3^{2-}) group is assigned to the positive band at 1124 cm^{-1} (*33*). The symmetric stretching vibration of the α and β (PO_2^-) is assigned to the band at 1094 cm^{-1}. The vibrations of all three phosphates are strongly coupled.

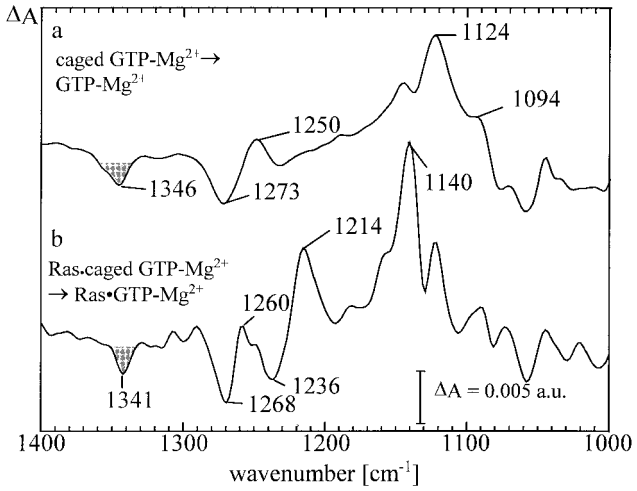

FIGURE 2: (a) Photolysis difference spectrum of 20 mM free caged GTP, 50 mM $MgCl_2$, 100 mM HEPES, pH 7.5. (b) Photolysis difference spectrum of 10 mM Ras-bound caged GTP, 25 mM $MgCl_2$, 10 mM DTT, 50 mM HEPES, 1% glycerol, pH 7.5.

Photolysis of Ras•caged GTP−Mg^{2+} *(Reaction* ***A****, Scheme 1).* The photolysis spectra of Ras-bound caged GTP is presented in Figure 2b. The shape of the Ras•caged GTP photolysis spectrum is remarkably different from the spectrum of free GTP (Figure 2a). The difference band of the free nucleotide at 1273/1250 cm^{-1} is split into two difference bands at 1268/1260 cm^{-1} and 1236/1214 cm^{-1} in the Ras-bound form. The broad positive band which is observed around 1124 cm^{-1} for GTP is shifted to 1140 cm^{-1} for the Ras-bound GTP. Below 1050 cm^{-1}, only some small bands are observed. As compared to the photolysis spectrum of free GTP, the phosphate bands gain intensity and are shifted to higher wavenumbers. Because the degrees of freedom of the nucleotide are reduced by binding to the protein, the bands become sharper (*25*, *33*).

The photolysis difference spectra of the Ras-bound unlabeled, **1**, and labeled caged GTP, **2**, **3**, and **4**, are shown in Figure 3a. The positive bands represent Ras•GTP and the negative bands Ras•caged GTP. Knowledge of the frequencies of GTP bands appearing in the photolysis difference spectra allows the identification of GTP bands in

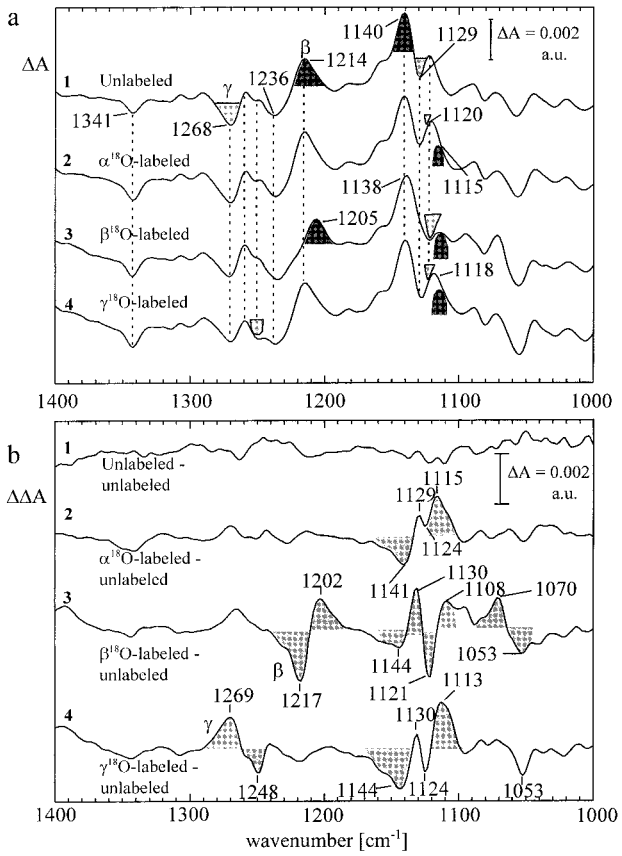

FIGURE 3: (a) Photolysis difference spectra of Ras-bound caged GTP, (**1**) unlabeled, (**2**) α^{18}O-labeled, (**3**) β^{18}O-labeled, (**4**) γ^{18}O-labeled. (b) Photolysis double differences spectra of Ras•caged GTP: between (**1**) unlabeled − unlabeled, (**2**) α^{18}O-labeled − unlabeled, (**3**) β^{18}O-labeled − unlabeled, and (**4**) γ^{18}O-labeled − unlabeled.

the hydrolysis difference spectra with Ras•GTP. The spectra are normalized to the band at 1341 cm^{-1}. This band represents the amount of photolyzed Ras•caged GTP. The shifted GTP bands are highlighted by dark shadings and the shifted caged GTP bands by light shadings. To visualize the band shifts, double difference spectra are performed (Figure 3b). They contain only the shifted bands, because all bands which are not affected by the labeling are subtracted. However, after localizing the shifts in the double difference spectra in Figure 3b, the wavenumber values used in the table for the respective phosphate vibrations are assigned in the difference spectra in Figure 3a.

As a control, the difference between photolysis spectra from two different unlabeled caged GTPs (**1**) is shown in trace 1 of Figure 3b. This indicates the quality of the baseline.

For Ras•caged GTPα^{18}O, **2**, the double difference spectrum is dominated by a negative band at 1141 cm^{-1} and a positive one at 1115 cm^{-1}. This difference band is superimposed by an additional smaller difference band at 1129/1124 cm^{-1}. Because the spectrum of the unlabeled compound has been subtracted, the negative band at 1141 cm^{-1} represents a downshift of a positive, i.e., GTP, band. The band pattern with two minima at 1141 and 1124 cm^{-1} and two maxima at 1129 and 1115 cm^{-1} can be caused by two different isotope shifts. Either we observe a shift of two subsequent GTP bands from 1141 to 1129 and 1124 to 1115 cm^{-1} which partly overlap, or a larger downshift of a GTP band from 1141 to 1115 cm^{-1} and a second superimposed smaller shift of a caged GTP band from 1129 to 1124 cm^{-1}. The α (PO_2^-) GTP band for free GTP shows a downshift of 30 cm^{-1} due to ^{18}O labeling (*33*). Therefore the latter explanation, the downshift from 1141 to 1115 cm^{-1}, is much more reasonable. We conclude that the shifted band at 1141 cm^{-1} in Figure 3 b represents the contribution of the symmetric stretching vibration of the α (PO_2^-) group. Similar shifts at 1141 cm^{-1} are also detected for the *β*- and *γ*-labeled caged GTP in traces **3** and **4**. Also the 1129/1124 cm^{-1} difference band shows shifts for the *β*- and *γ*-labeled nucleotide. Because the 1129/1124 cm^{-1} difference band is more pronounced in traces **3** and **4**, it will be discussed below.

For Ras•caged GTPβ^{18}O, **3**, (Figure 3b), additional isotope shifts as compared to Ras•caged GTPα^{18}O are seen. A pronounced GTP band shifts from 1217 to 1202 cm^{-1} (compare also Figure 3a, traces **1** and **3**). Thus, the band at 1217 cm^{-1} must be assigned to the asymmetric stretching vibration of the *β* phosphate of GTP. A further GTP band shifts from about 1144 to about 1108 cm^{-1}, similar to that in trace **2**. The shifted band at 1144 cm^{-1} represents the contribution of the symmetric stretching vibration of the GTP *β* (PO_2^-) moiety to this band. The shift of the caged GTP band from 1130 to 1121 cm^{-1} has higher intensity than in trace **2** and masks therefore the band at 1144 cm^{-1} partly. The shifted band at 1130 cm^{-1} represents the contribution of the symmetric stretching vibration of the *β* (PO_2^-) groups of caged GTP. Finally, a shift from 1070 to 1053 cm^{-1} is observed which can be explained as a symmetric stretching vibration of the *β* (PO_2^-) group belonging to caged GTP. We propose that the first band at 1130 cm^{-1} is the in-phase symmetric stretching mode, while the latter band at 1070 cm^{-1} is due to the out-of-phase stretching mode. It is interesting that the out-of-phase mode has significant intensity in the IR spectra.

In the photolysis spectrum of Ras•caged GTPγ^{18}O, **4**, a band shift is observed from 1269 to about 1248 cm^{-1}. The band at 1269 cm^{-1} represents the asymmetric stretching vibration of the *γ* (PO_2^-) moiety of caged GTP. In the lower spectral region, again a GTP band shift from 1144 to 1113 cm^{-1} is observed as in traces **2** and **3**. It represents the contribution of the *γ* (PO_3^{2-}) degenerate stretching mode to the band at 1140 cm^{-1}. The difference band at 1130/1124 cm^{-1} is again superimposed, as in traces **2** and **3**, representing the contribution of the symmetric *γ* (PO_2^-) vibration of caged GTP. Since the symmetric (PO_2^-) stretching vibrations of caged GTP at 1130 cm^{-1} are shifted by all labels, the vibration is largely coupled among the α-, *β*-, and *γ*-phosphates.

In summary, the photolysis spectra of Ras•caged GTP show in comparison to the spectra of free caged GTP a lower degree of coupling among the phosphate groups. In the photolysis spectra of free caged GTP, similar isotope shifts were observed for all labels used in both spectral regions, between 1300 and 1200 cm^{-1} and between 1150 and 1050 cm^{-1} (*33*). In Ras•caged GTP photolysis spectra, between 1300 and 1200 cm^{-1}, a *β* GTP band is assigned at 1214 cm^{-1} and a *γ* caged GTP band at 1268 cm^{-1} is observed. Between 1150 and 1050 cm^{-1}, a GTP band at 1140 cm^{-1} and a caged GTP band at 1129 cm^{-1} are observed which react with all labels used and represent coupled vibrations (Figure 3a).

Table 1: Overview of the Assigned Phosphate Vibrations (in cm^{-1}) of Free and Ras-Bound Caged GTP, GTP, and GDP in Photolysis Difference Spectra and Hydrolysis Difference Spectra[a]

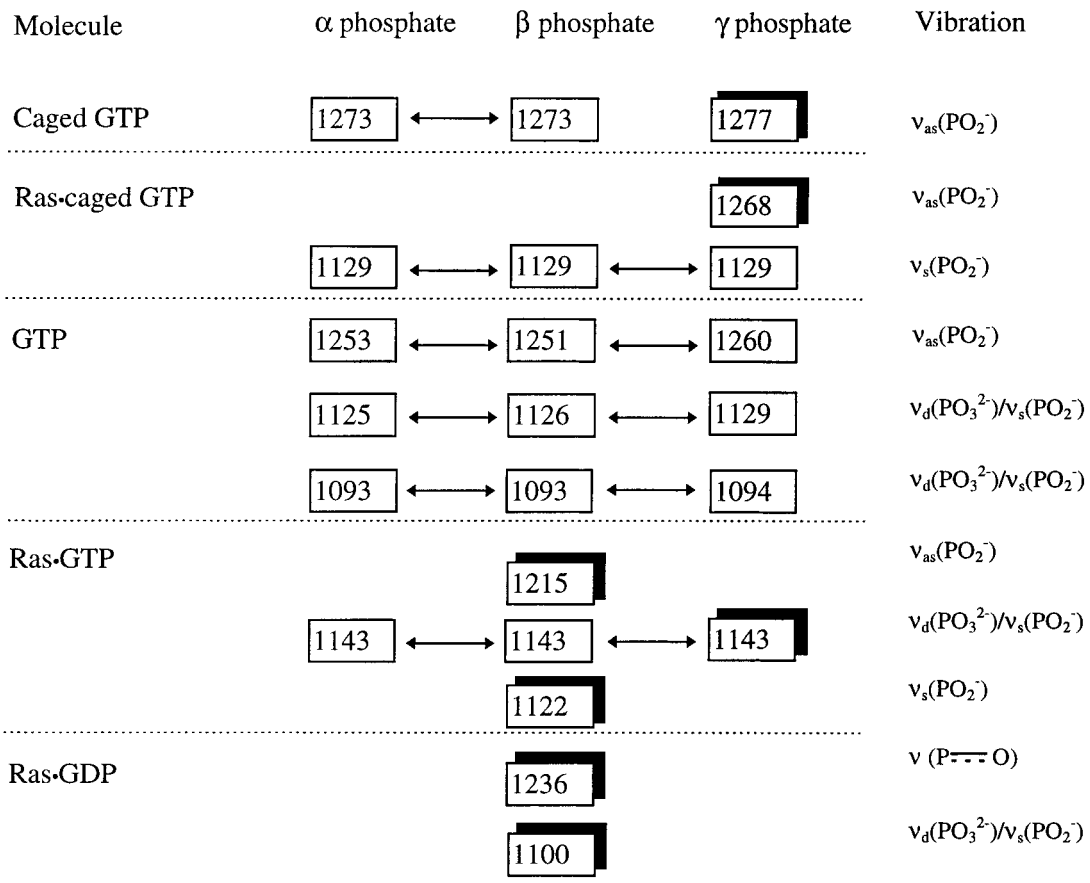

[a] Coupled vibrations are marked by double arrows, and the isolated vibrations which can serve as marker bands are highlighted. The wavenumber values for Ras•GTP are taken from the hydrolysis difference spectra, and those for free caged GTP and GTP are taken from Cepus et al. (*33*).

However, the γ-phosphate group contributes most to the band at 1140 cm^{-1}, and the β-phosphate group contributes most to the band at 1129 cm^{-1}. The results for the phosphate band assignments are summarized in Table 1.

As compared to vibrations of free GTP, in the Ras-bound case, the GTP β (PO_2^-) vibration shows the largest deviation. In free GTP, the asymmetric (PO_2^-) vibration absorbs at 1251 cm^{-1} and is strongly coupled among all three phosphates (Table 1). On binding to Ras, it is downshifted by 37 cm^{-1} to 1214 cm^{-1} and represents an isolated β-vibration. The frequency downshift indicates a dramatic decrease in the bond order of the β (PO_2^-) group. The importance of this observation will be discussed below.

*Intrinsic GTPase Reaction of Ras•GTP−Mg^{2+} (Reaction **B**, Scheme 1).* The photolysis reaction of the Ras•caged GTP complex yields Ras•GTP. Because caged GTP is already bound to Ras in the correct conformation (*36*), the GTPase reaction is directly started.

The first FTIR spectrum measured immediately after complete photolysis of Ras•caged GTP represents Ras•GTP. This spectrum is used as a reference spectrum and subtracted from the following spectra, including those that are recorded during the enzymatic GTP hydrolysis. As examples, three difference spectra out of a set of 100, taken at 6, 20, and 40 min after photolysis, are presented in Figure 4a. Positive bands in the absorbance difference spectra represent Ras•GDP and inorganic phosphate, and negative bands represent Ras•GTP. The GTPase spectrum shows a large difference band in the amide I region at 1664/1635 cm^{-1}. In the amide II region, difference bands are detected at 1577, 1556, 1545, 1520, and 1510 cm^{-1}. In the phosphate vibrational region, pronounced positive bands can be observed at 1236, 1100, and 1078 cm^{-1}, and negative bands at 1260, 1215, 1143, and 1122 cm^{-1}. The phosphate absorbance changes can be largely explained by the loss of the β (PO_2^-) group, which is converted to the terminal β (PO_3^{2-}) moiety of GDP, and the loss of the former terminal γ (PO_3^{2-}) group of GTP, which is hydrolyzed to inorganic phosphate. These conversions of phosphate groups lead to a decreased bond order of the former β and γ phosphate groups of GTP. Due to the bond order decrease, the bands are shifted to lower wavenumbers.

Typical time courses of the bands at 1236 and 1143 cm^{-1} are shown in Figure 4b. The absorbance changes at the respective times and the fitted curves are shown. The kinetic analysis yields a rate constant of $k = 0.018$ min^{-1}, in agreement with published data obtained with other techniques (*37*, *38*).

For the assignments of phosphate bands, the GTP isotopomers which originate from the ^{18}O-labeled caged GTP are used. The spectra of the GTPase reaction using the isotopomers, **1′**, **2′**, **3′**, and **4′**, are shown in Figure 5a. The spectra

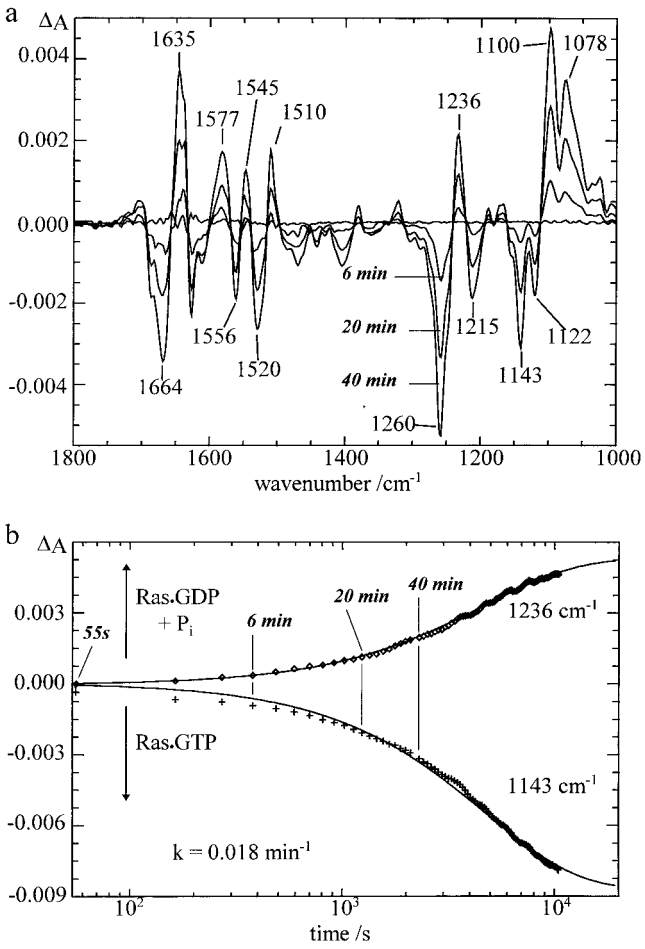

FIGURE 4: (a) Difference spectra of the Ras•GTP hydrolysis reaction, recorded at 6, 20, and 40 min after photochemical initiation; the flat baseline represents the difference between two spectra taken before the flash to control the baseline quality. The Ras•GTP spectrum (the first spectrum taken after the photolytic release of GTP) is subtracted from the spectra acquired during the GTPase reaction. (b) Time course of the absorbance changes at 1236 and 1143 cm^{-1}, indicating the disappearing GTP and the appearing GDP and P_i. A global fit analysis yields $k = 0.018$ min^{-1}, in agreement with published data.

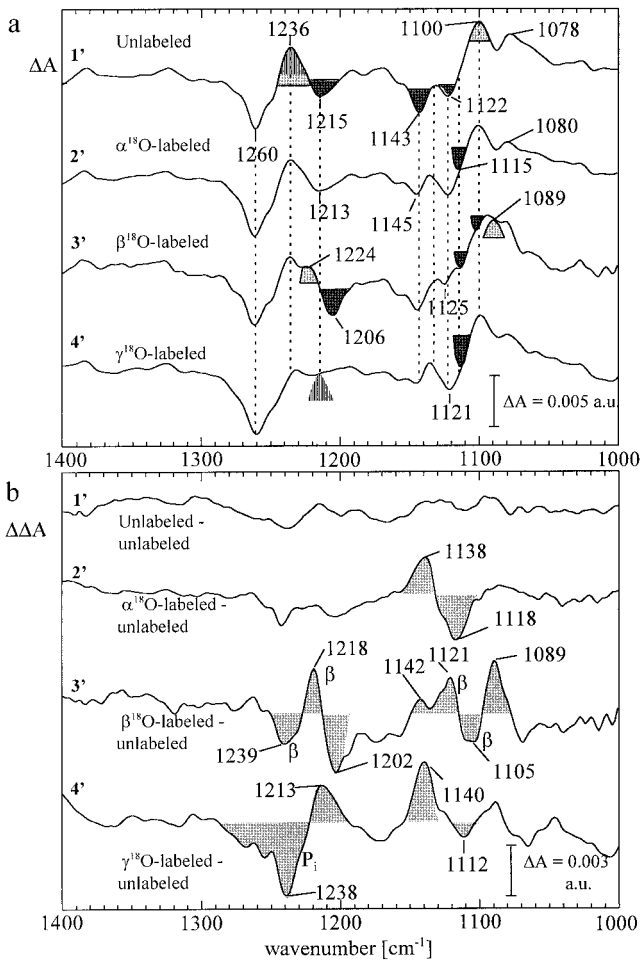

FIGURE 5: (a) Hydrolysis difference spectra of Ras•GTP: (**1′**) unlabeled, (**2′**) $\alpha^{18}O$ labeled, (**3′**) $\beta^{18}O$ labeled, and (**4′**) $\gamma^{18}O$ labeled. (b) Hydrolysis double difference spectra of Ras•GTP: (**1′**) between unlabeled − unlabeled, (**2′**) $\alpha^{18}O$ labeled − unlabeled, (**3′**) $\beta^{18}O$ labeled − unlabeled, and (**4′**) $\gamma^{18}O$ labeled − unlabeled.

are normalized to the bands appearing between 1800 and 1400 cm^{-1}, where no change due to the isotope labeling should occur. The isotopic shifts are visualized again in the double differences shown in Figure 5b. The shifts of GDP bands are highlighted by light shading and those of GTP bands by dark shading. The shift caused by the inorganic phosphate is highlighted by the striped area. The Ras•GTP bands, observed in the hydrolysis difference spectra, should agree with the Ras GTP•bands assigned already in the photolysis difference spectra. In contrast to the photolysis difference spectra, the GTP phosphate bands are negative, because in the hydrolysis difference spectra they represent the educt. However, the same isotope shifts are expected for the GTP phosphate vibrations.

Using α-labeled GTP, **2′**, a GTP band shifts from 1138 to 1118 cm^{-1} (Figure 5b). Similar shifts from 1141 to 1115 cm^{-1} were identified already in the photolysis difference spectra (Figure 3b). This band is assigned in the photolysis difference spectra to a coupled vibration of the α and β (PO_2^-) and the γ (PO_3^{2-}) groups (Table 1).

The spectrum of the GTPase reaction of $\beta^{18}O$-labeled GTP, **3′**, yields additional shifts. The difference spectrum reflects a disappearing β (PO_2^-) group and an appearing β (PO_3^{2-}) group. A GDP band shifts from 1239 to about 1218 cm^{-1}. The band at 1239 cm^{-1} must represent the appearing β (PO_3^{2-}) group. A second shift is superimposed from about 1218 to 1202 cm^{-1}, already observed in the photolysis difference spectra (Figure 3b, trace **3**). The band at 1218 cm^{-1} represents the asymmetric stretching vibration of the GTP β (PO_2^-) group (Table 1). A further GTP band shifts from 1142 cm^{-1}. The exact downshift cannot be determined because two further isotope shifts are superimposed. The first one is a GTP band shift from 1121 to about 1105 cm^{-1}. It represents an isolated symmetric stretching vibration of the β (PO_2^-) moiety. This was not obvious in the photolysis difference spectra. The second one is a GDP band shift from about 1105 to 1089 cm^{-1}. This band can be assigned to a degenerate stretching vibration of the β (PO_3^{2-}) group. Even if only one β-oxygen is isotopically labeled, vibrations of different P−O bonds may be shifted due to vibrational coupling.

The spectrum of the $\gamma^{18}O$-labeled isotopomer, **4′**, is less complex. While in the GTP bound form the label is in the γ-position of the triphosphate chain, after hydrolysis the GDP is unlabeled, having released an ^{18}O-labeled inorganic phosphate. Only one of the four oxygens of the free phosphate is labeled. We observe mainly a shift of a positive

band from 1238 to 1213 cm^{-1}. This can only be assigned to a vibration of the inorganic phosphate since the other hydrolysis product, GDP, is unlabeled. The high frequency indicates a P−O−H in-phase bending vibration of a doubly protonated inorganic phosphate (*39*). This assignment is supported by pH titration experiments (V. Cepus et al., unpublished). Spectra of the GTPase reaction have been recorded between pH 5 and pH 9. The band at 1236 cm^{-1} decreases with the rising pH, indicating a decreasing concentration of $H_2PO_4^-$ (data not shown). We determined the p*K* value of the system $H_2PO_4^-/HPO_4^{2-}$ to be around 6.8, the same as in solution. At the measuring conditions of pH 7.5, the singly protonated phosphate dominates (ca. 80%). However, HPO_4^{2-} has a very broad band of about 200 cm^{-1} located below 1200 cm^{-1} with smaller extinction coefficients and is therefore not reflected in the difference spectra with specific single bands.

Furthermore, a GTP band shifts from 1140 cm^{-1} to about 1112 cm^{-1} (Figure 5b, trace **4′**) as in the photolysis difference spectra, representing the contribution of the γ (PO_3^{2-}) group to the coupled GTP vibration at 1139 cm^{-1}. The γ-phosphate contributes most to this band and can serve as a marker band for GTP hydrolysis.

A summary of the phosphate band assignments is presented in Table 1. Again, most remarkable are GDP β-phosphate vibrations.

The β P−O vibrations of Ras-bound GDP absorb at 1236 and 1100 cm^{-1}. The P−O vibration of the β (PO_3^{2-}) group of free ADP•Mg can be used as reference. It has a binding order of 1.3 and absorbs at 1121 cm^{-1} (*40*). Therefore, for symmetrically distributed electrons in the β (PO_3^{2-}) group of Ras-bound GDP, a phosphate band at 1121 cm^{-1} is expected. However, we observe one of the β-phosphate bands at 1236 cm^{-1}. This is even 16 cm^{-1} higher than the P−O vibration of the α (PO_2^-) group of free ADP•Mg with a binding order of 1.5. The band at 1236 cm^{-1} indicates therefore a β P−O vibration of a phosphate group with a bond order of significantly higher than 1.5. On the other hand, the second β P−O vibration at 1100 cm^{-1} is 21 cm^{-1} downshifted, as compared to the frequency of symmetrically distributed electrons in a (PO_3^{2-}) group. The lower frequency indicates a bond order significantly lower than 1.3.

From these assignments we conclude that the electrons are not symmetrically distributed and two different species of P−O bonds are present in the β-phosphate group. The comparison between the bands at 1236 and 1100 cm^{-1} shows a higher intensity for the second band. A comparison of the integral intensities of the bands at 1236 and 1100 cm^{-1} shows that the latter is ca. 1.6 timer larger than the former. To avoid distortions due to overlapping bands, the integral intensity is not taken directly at 1100 cm^{-1}, but of the shifted band at 1089 cm^{-1} of the β^{18}O-labeled sample. Because the band at 1100 cm^{-1} is, within experimental error, about 2 times larger than the band at 1236 cm^{-1}, the former appears to represent two P−O bonds and the latter one P−O bond. Small deviations in the extinction coefficients and uncertainties in the determination of the integral intensity may reduce the expected factor of 2 to 1.6.

CONCLUSIONS

What Can Be Learned from the Assignments of the Phosphate Bands for the GTPase Mechanism of Ras? The asymmetric GTP β (PO_2^-) vibration at 1215 cm^{-1} in the Ras-bound case has an unexpectedly low value. This downshift, in comparison with unbound GTP, indicates a large decrease in the P−O bond order. Such a decrease can be explained by a strong interaction of the β (PO_2^-) oxygen atoms with the protein, which renders the β-phosphorus electron deficient. Because of this, electrons will be withdrawn from the oxygen atom, bridging the β- and γ-phosphorus atoms, thus weakening the bond to the γ-phosphate. The protein interacts strongly with the β-phosphate in order to preprogram the splitting into GDP and inorganic phosphate in the subsequent GTPase reaction.

For Ras-bound GDP, the β-phosphate bands have been assigned at 1236 and 1100 cm^{-1}. The unusually high frequency of the smaller band at 1236 cm^{-1} indicates a single P−O group with a significantly higher bond order than 1.5. This is assigned to the former β/γ-bridging oxygen which, after bond cleavage, forms nearly a double bond to the β-phosphorus atom. The unusually low wavenumber of the band at 1100 cm^{-1}, with larger intensity, indicates two P−O groups with a significantly lower bond order than 1.3. Therefore, the other two oxygen atoms of the β (PO_3^{2-}) moiety remain strongly coordinated by the Ras protein, in a similar way as in the Ras•GTP state. However, to make more quantitative conclusions, a detailed normal-mode analysis of the phosphate vibrations has to be performed. This work is in progress. The decoupling of phosphate vibrations may also contribute to the downshifts.

The GTP γ-phosphate vibration at 1143 cm^{-1} is 17 cm^{-1} upshifted in the protein as compared to free GTP. This indicates an increase in bond order of the γ (PO_3^{2-}) group. Therefore, at least one of the two γ-phosphate oxygens, which do not interact with the magnesium ion, is more weakly bound to the protein than the β-phosphate oxygens.

Are the Results Compatible with the X-ray Structural Models of Ras? In the X-ray structures of Ras with a slowly hydrolyzing GTP analogue, GppNHp, multiple interactions of the β- and the γ-phosphate groups were identified, which would result in strong binding of both β- and γ-phosphates to Ras (*12*, *13*, *41*). The most important interactions from the X-ray structural model (*13*) are presented in Figure 6a. However, there are more interactions with the NH bonds of the P-loop peptide groups and they appear to form a positive electrostatic field in whose center the β-phosphate is located (*13*). Moreover, the interactions with the β-phosphate groups are better defined than with the γ-phosphate due to lower B factors of the surrounding protein. The FTIR results discriminate now between the coordination strength of the β- and the γ-phosphate. They show a much stronger binding of the β-phosphate than of the γ-phosphate to the protein.

In contrast to the proposed X-ray structural model, electron spin−echo envelope modulation spectroscopy shows that Thr-35 seems not to be coordinated to the divalent metal ion and therefore presumably does not interact with the γ-phosphate in solution (*42*). This will also cause a weaker γ-phosphate binding which is generally in agreement with our results. However, the discrepancy between this result and the X-ray result suggests that in the crystal structure, a minor conformation has been trapped, which is maybe an important one, and perhaps the predominant one for GTP,

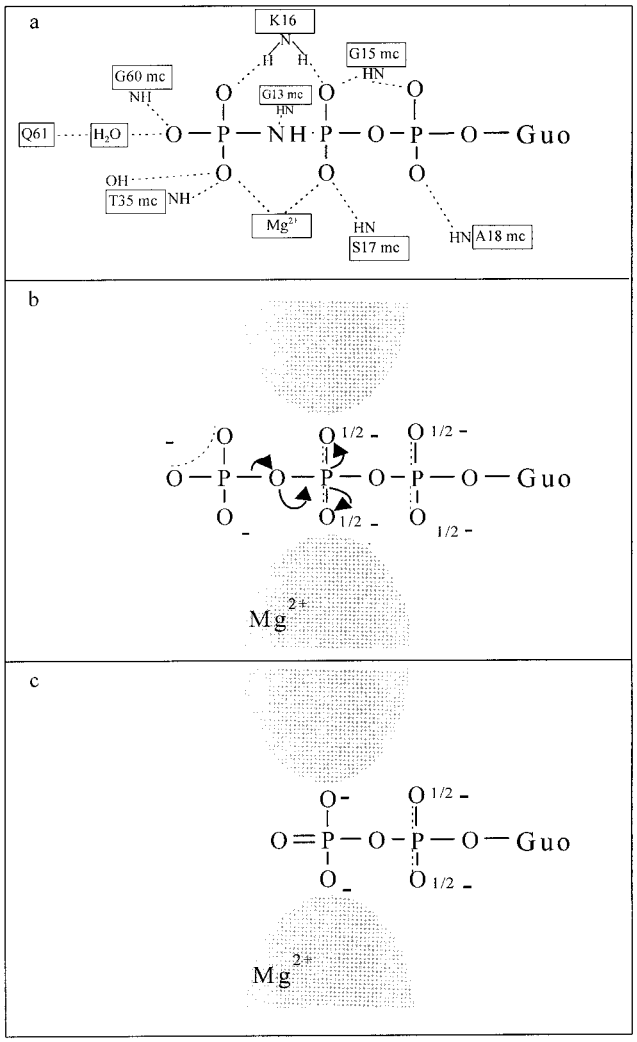

FIGURE 6: (a) X-ray structural model of Ras•GppNHp showing H bonds shorter than 3.1 Å, the catalytically active water, and the important residue Gln-61 [modified figure, taken from Wittinghofer and Pai (*13*)]. The γ-phosphate forms H-bonds to three amino acids belonging to the P-loop (L1; ca. amino acids 9−15), the effector binding or switch I region (L2; 30−40), and the switch II region (L4; 59−65), respectively. However, the temperature factors in the switch II region have values up to 54.1 $Å^2$, reflecting the high flexibility of L4 in the environment of the γ-phosphate. The β-phosphate is similarly well bound by the protein. H-bonds are formed mainly to the main chain NH groups of the P-loop peptide bonds. Four amino acids can be counted which are involved in the coordination of the β-phosphate. Additionally, one magnesium ion is located symmetrically between the β- and γ-phosphate, and is thus an important factor in localizing the phosphate groups. Summarizing the X-ray structural models for Ras•GppNHp, in principle both the β- and γ-phosphate are well bound to Ras. b) Interaction model of Ras•GTP, consistent with FTIR spectroscopic results; the shadows indicate the "protein finger" which especially stabilizes the β-phosphate of GTP, pulling electron density toward it and thereby weakening the bridging $P_\gamma-O_{\beta/\gamma}$ bond. (c) Interaction model of Ras•GDP; the strong interaction of the "protein finger" (gray shading) to the nucleotide remains very strong, leading to a favorable localization of a double bond of the formerly bridging $O_{\beta/\gamma}-P_\beta$ bond (Guo = guanosine).

rather than GppNHp, which was used for this EPR study. Furthermore, for Ras•GDP, EPR experiments and the crystal structure reveal a coordination of the β-phosphate to magnesium but not of the α-phosphate (*43, 44*). This also agrees nicely with the FTIR results of a strong GDP β-phosphate binding to Ras.

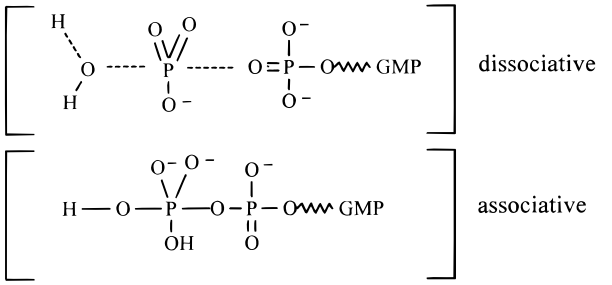

FIGURE 7: Proposed structures for a dissociative and an associative transition state in the course of GTP hydrolysis.

Do the Presented Results Now Favor a Dissociative or an Associative Transition State? In a dissociative transition state, negative charge is accumulated at the β-phosphate and the binding order of the γ-phosphate increases, leading to a metaphosphate-like intermediate. In contrast, in an associative transition state, the charge accumulates at the pentavalent γ-phosphate and its binding order is decreased (Figure 7). Thus, important criteria for a GTP hydrolysis mechanism via a dissociative transition state are a strong binding of the β-phosphate and a weakening of the bond between the β- and γ-phosphate. Therefore, the strong interaction of the β-phosphate with the protein points toward a dissociative mechanism (Figure 7). Although we have not recorded FTIR difference spectra of the transition state itself, it seems very likely that the strong interaction of the β-phosphate in GTP and GDP is also characteristic of the transition state.

Does the Stabilization of Negative Charge on the β-Phosphate Exclude an Associative Mechanism? The negative charge stabilization at the β-phosphate may also increase the susceptibility of the γ-phosphate to be attacked by a nucleophile because of the general tendency for electrons to be pulled toward the β-phosphate. The weakening of the β/γ-bridging $P_\gamma-O$ bond is not necessarily anticatalytic for further events more characteristic of an associative mechanism, since it should also increase the susceptibility of the γ-phosphate to be attacked by a nucleophile. The preceding protonation of the γ-phosphate, as suggested by Schweins et al. may contribute to stabilization of a pentacovalent intermediate in an associative mechanism (*16*). Support for an associative mechanism of the GAP catalyzed GTPase reaction of Ras and Rho has been obtained from the putative transition state analogues GDP•AlF_3 or GDP•AlF_4^- (*17, 18*). The authors identified an essential Arg in the GAP catalyzed reaction which is able to effectively stabilize the negative charge of a proposed pentacovalent γ-phosphate. However, there might be differences between the intrinsic GTPase mechanism and the GAP catalyzed mechanism. This will be investigated in further time-resolved FTIR studies on the GAP catalyzed GTPase mechanism.

In summary, we suggest that there is a significant contribution of the weakening of the β/γ-bridging $P_\gamma-O$ bond caused by the strong interaction of the β-phosphate with the protein environment, which preprograms the splitting. The enzyme seems to make use of features of both dissociative and associative mechanisms.

The results presented here establish time-resolved FTIR difference spectroscopy as a new tool for nonchromophoric proteins which can provide new insights into the GTPase mechanism of Ras, complementary to the X-ray structure analysis. The specific phosphate marker bands will be useful

tools for further time-resolved FTIR investigations of the GTPase mechanism of Ras, including oncogenic Ras mutants. In the next step, the protein−protein interactions between Ras on one hand and its effector Raf kinase or its regulator GAP will be investigated. Furthermore, this approach can be extended to other GTPases and ATPases.

In comparison with X-ray structure analysis, FTIR studies can be performed more rapidly and in solution. The crystallization process and the use of GTP analogues can also have an effect on the protein structure. Starting with the ground-state structural models obtained by X-ray analysis, the complementary FTIR data can contribute to an improvement of the structural resolution, for example by resolving H-bonds and internal water molecules (*45*). In particular, the active site temperature factors in X-ray structures are often high, and the resulting models are less reliable in these regions. However, the main advantage of FTIR studies is the high time-resolution by which molecular reactions are monitored in real time.

ACKNOWLEDGMENT

We thank Marija Matuska for the excellent technical assistance and Christoph Allin and Dr. Alfred Wittinghofer for very useful discussions.

REFERENCES

1. McCormick, F. (1993) *Nature 363*, 15−16.
2. Li, N., Batzer, A., Yajnik, V., Skolnik, E., Chardin, P., Bar-Sagi, D., Margolis, B., and Schlessinger, J. (1993) *Nature 363*, 85−88.
3. Wiesmüller, L., and Wittinghofer, F. (1994) *Cell. Signalling 6*, 247−267.
4. John, J., Schlichting, I., Schiltz, E., Rösch, P., and Wittinghofer, A. (1989) *J. Am. Chem. Soc. 264*, 13086−13092.
5. Bourne, H. R., Sanders, D. W., and McCormick, F. (1990) *Nature 348*, 125−132.
6. Lowy, D. R., and Willumsen, B. M. (1993) *Annu. Rev. Biochem. 62*, 851−891.
7. Gideon, P., John, J., Frech, M., Lautwein, A., Clark, R., Scheffler, J. E., and Wittinghofer, A. (1992) *Mol. Cell. Biol. 12*, 2050−2056.
8. Der, D., Finkel, T., and Cooper, G. M. (1986) *Cell 44*, 167−176.
9. Barbacid, M. (1987) *Annu. Rev. Biochem. 56*, 779−827.
10. Levitzki, A. (1994) *Eur. J. Biochem. 226*, 1−13.
11. Pai, E. F., Kabsch, W., Krengel, U., Holmes, K. C., John, J., and Wittinghofer, A. (1989) *Nature 341*, 209−214.
12. Pai, E. F., Krengel, U., Petsko, G. A., Goody, R. S., Kabsch, W., and Wittinghofer, A. (1990) *EMBO J. 9*, 2351−2359.
13. Wittinghofer, A., and Pai, E. F. (1991) *Trends Biochem. Sci. 16*, 382−386.
14. Frech, M., Darden, T. A., Pedersen, L. G., Foley, C. K., Charifson, P. S., Anderson, M. W., and Wittinghofer, A. (1994) *Biochemistry 33*, 3237−3244.
15. Chung, H.-H., Benson, D. R., and Schultz, P. G. (1993) *Science 259*, 806−809.
16. Schweins, T., Geyer, M., Scheffzek, K., Warshel, A., Kalbitzer, H. R., and Wittinghofer, A. (1995) *Nat. Struct. Biol. 2*, 36−44.
17. Scheffzek, K., Ahmadian, M. R., Kabsch, W., Wiesmüller, L., Lautwein, A., Schmitz, F., and Wittinghofer, A. (1997) *Science 277*, 333−338.
18. Rittinger, K., Walker, P. A., Eccleston, J. F., Smerdon, S. J., and Gamblin, S. J. (1997) *Nature 389*, 758−762.
19. Sondek, J., Lambright, D. G., Noel, J. P., Hamm, H. E., and Sigler, P. B. (1994) *Nature 372*, 276−279.
20. Coleman, D. E., Berghuis, A. M., Lee, E., Linder, M. E., Gilman, A. G., and Sprang, S. R. (1994) *Science 265*, 1405−1412.
21. Maegley, K. A., Admiraal, S. J., and Herschlag, D. (1996) *Proc. Natl. Acad. Sci. U.S.A. 93*, 8160−8166.
22. Gerwert, K. (1993) *Biochim. Biophys. Acta 1101*, 147−153.
23. Gerwert, K., Souvignier, G., and Hess, B. (1990) *Proc. Natl. Acad. Sci. U.S.A. 87*, 9774−9778.
24. Brudler, R., de Groot, H. J. M., van Liemt, W. B. S., Steggerda, W. F., Esmeijer, R., Gast, P., Hoff, A. J., Lugtenburg, J., Gerwert, K. (1994) *EMBO J. 13*, 5523−5530.
25. Gerwert, K., Cepus, V., Scheidig, A., and Goody, R. S. (1994) in *Time-Resolved Vibrational Spectroscopy VI* (Lau, A., Siebert, F., and Werncke, W., Eds.) pp 185−187, Springer-Verlag, Berlin, Heidelberg.
26. Schlichting, I., Rapp, G., John, J., Wittinghofer, A., Pai, E. F., and Goody, R. S. (1989) *Proc. Natl. Acad. Sci. U.S.A. 86*, 7687−7690.
27. Schlichting, I., Almo, S. C., Rapp, G., Wilson, K., Petratos, K., Lentfer, A., Wittinghofer, A., Kabsch, W., Pai, E. F., Petsko, G. A., and Goody, R. S. (1990) *Nature 345*, 309−315.
28. Walker, J., Reid, G. P., McCray, J. A., and Trentham, D. R. (1988) *J. Am. Chem. Soc. 110*, 7170−7177.
29. Kalbitzer, H. R., Feuerstein, J., Goody, R. S., and Wittinghofer, A. (1990) *Eur. J. Biochem. 188*, 355−359.
30. John, J., Sohmen, R., Feuerstein, J., Linke, R., Wittinghofer, A., and Goody, R. S. (1990) *Biochemistry 29*, 6058−6065.
31. Gerwert, K, Souvignier, G., and Hess, B. (1990) *Proc. Natl. Acad. Sci. U.S.A. 87*, 9774−9778.
32. Hessling, B., Herbst, J., Rammelsberg, R., and Gerwert, K. (1997) *Biophys. J. 73*, 2071−2080.
33. Cepus, V., Allin, C., Ulbrich, C., Troullier, A., and Gerwert, K. (1998) in *Methods in Enzymology, Vol. 291* (Mariott, G., Ed.) pp 223−245, Academic Press, San Diego.
34. Barth, A., Hauser, K., Mäntele, W., Corrie, J. E. T., and Trentham, D. R. (1995) *J. Am. Chem. Soc. 117*, 10311−10316.
35. Colthup, N. B., Daly, L. H., and Wiberley, S. E. (1990) *Introduction to Infrared and Raman Spectroscopy*, Academic Press, San Diego. Inc.
36. Scheidig, A. J., Franken, S. M., Corrie, J. E. T., Reid, G. P., Wittinghofer, A., Pai, E. F., and Goody, R. S. (1995) *J. Mol. Biol. 253*, 132−150.
37. Krengel, U., Schlichting, I., Scherer, A., Schumann, R., Frech, M., John, J., Kabsch, W., Pai, E. F., and Wittinghofer, A. (1990) *Cell 62*, 539−548.
38. Schweins, T., Geyer, M., Kalbitzer, H. R., Wittinghofer, A., and Warshel, A. (1996) *Biochemistry 35*, 14225−14231.
39. Chapman, A. C., and Thirlwell, L. E. (1964) *Spectrochim. Acta 20*, 937−947.
40. Takeuchi, H., Murata, H., and Harada, I. (1988) *J. Am. Chem. Soc. 110*, 392−397.
41. Milburn, M. V., Tong, L., de Vos, A. M., Brünger, A., Yamaizumi, Z., Nishimura, S., and Kim, S.-H. (1990) *Science 247*, 939−945.
42. Farrar, C. T., Halkides, C. J., and Singel, D. J. (1997) *Structure 5*, 1055−1066.
43. Feuerstein, J., Kalbitzer, H. R., John, J., Goody, R. S., and Wittinghofer, A. (1987) *Eur. J. Biochem. 162*, 49−55.
44. Tong, L., de Vos, A. M., Milburn, M. V., and Kim, S.-H. (1991) *J. Mol. Biol. 217*, 503−516.
45. le Coutre, J., Tittor, J., Oesterhelt, D., and Gerwert, K. (1995) *Proc. Natl. Acad. Sci. U.S.A. 92*, 4962−4966.

BI973183J